

1 **Genetic editing of *CISH* enhances T cell effector programs independently of**
2 **immune checkpoint cell surface ligand expression**

3
4
5 Elisa Arthofer¹, Krishnendu Chakraborty¹, Lydia Viney¹, Matthew J Johnson^{2,3,4}, Beau R.
6 Webber^{2,3,4}, Branden S. Moriarity^{2,3,4}, Emil Lou⁵, Modassir Choudhry¹, Christopher A.
7 Klebanoff^{6,7}, Tom Henley⁵

8
9 ¹Intima Bioscience, New York, USA.

10 ²Masonic Cancer Center, University of Minnesota, Minneapolis, MN, USA

11 ³Center for Genome Engineering, University of Minnesota, Minneapolis, MN, USA

12 ⁴Department of Pediatrics, University of Minnesota, Minneapolis, MN, USA

13 ⁵Department of Medicine, Division of Hematology, Oncology and Transplantation, University
14 of Minnesota, Minneapolis, MN, USA.

15 ⁶Human Oncology and Pathogenesis Program, Immuno-oncology Service, Memorial Sloan
16 Kettering Cancer Center (MSKCC), New York, NY, USA.

17 ⁷Center for Cell Engineering, MSKCC, New York, NY, USA.

18
19
20 ⁵Co-corresponding Authors:

21 Tom Henley, tom@intimabioscience.com;

22 Christopher A. Klebanoff, klebanoc@mskcc.org;

23

24

25

26

27

28

29

30

31 **ABSTRACT**

32 PD-1 acts as a negative regulator of T cell-mediated immune responses in the setting of persistent
33 antigen expression, including cancer and chronic pathogen infections. Antibody-mediated blockade of
34 the PD-1/PD-L1 axis benefits a subset of patients with highly immunogenic malignancies; however,
35 many patients fail to respond due to a requirement for expression of the cell surface ligand PD-L1
36 within the tumor microenvironment. CISH is a member of a new class of intra-cellular immune
37 checkpoint molecules that function downstream of the T cell receptor to regulate antigen-specific
38 effector functions, including reactivity to cancer neoantigens. Herein, we employed multiplex CRISPR
39 editing of primary human T cells to systematically compare the function of *CISH* deletion relative to
40 *PDCD1* (the gene encoding PD-1) and/or *VSIG9* (the gene encoding TIGIT) in a model of neoantigen-
41 mediated cancer cell cytolysis. PD-1 and TIGIT disruption enhanced cytolytic activity exclusively in the
42 setting of high PD-L1 expression. In contrast, CISH inactivation enhanced antigen-specific cytolysis of
43 tumor cells regardless of PD-L1 expression, including outperforming PD-1 and TIGIT disruption even
44 in the presence of high PD-L1 tumor cells. Furthermore, we observed a synergistic increase in tumor
45 cell killing when CISH and PD-1 or TIGIT are inactivated in combination, supporting the notion that
46 these immune checkpoints regulate non-redundant pathways of T cell activation. Together, these data
47 demonstrate that the intra-cellular immune checkpoint protein CISH can potentially enhance anti-
48 tumor responses against a broad range of cancer types regardless of PD-L1 biomarker status.

49

50 **Key words:** CRISPR, immune checkpoint, PD-1, PD-L1, TIGIT, immunotherapy, T Cell Therapy, TIL,
51 TCR, Cancer, CISH

52

53

54

55

56

57

58

59

60

61

62

63

64 **MAIN**

65

66 T cells play a crucial role in immune-mediated tumor clearance by recognizing tumor cells via their T
67 cell receptors (TCRs) to elicit a program of targeted destruction culminating in cancer cell lysis¹. A
68 critical requirement for improving clinical responses to immunotherapy lies in enhancing the
69 functional avidity of cancer antigen-specific T cells^{2, 3}. Thus, the field of immune checkpoint inhibition
70 has developed to advance the clinical outcomes of anti-cancer therapies via modalities to inhibit T cell
71 immune checkpoints and reduce the immunosuppressive effects these cells encounter⁴. Therapeutic
72 blockade of immune checkpoint receptors or their associated ligands, such as Programmed Cell Death
73 Protein 1 (PD-1) and PD-L1, can trigger the regression of diverse cancer types. These findings
74 underscore the potential of targeted approaches to enhance and prolong antigen-specific T cell
75 responses^{5, 6, 7, 8, 9, 10}.

76 The interaction of PD-1 with its ligands, programmed death 1 ligand (PD-L1) and PD-L2, inhibit
77 T cell activation, suppress proliferation, and limit anti-tumor effector functions through a co-inhibitory
78 signaling pathway^{11, 12}. FDA approved monoclonal antibody (mAb) inhibitors of PD-1 and PD-L1 have
79 shown impressive clinical outcomes in a subset of patients resulting in durable tumor regression and
80 extended progression free survival^{13, 14}. Despite these clinical successes, most patients show no
81 response to blockade of the PD-1/PD-L1 axis. Several mechanisms have been identified that underly
82 this resistance, most notably a requirement for cells in the tumor microenvironment (TME) to express
83 PD-L1^{5, 15, 16, 17}. PD-L1 expression within the TME can vary between patients and low or absent
84 expression can render the patient unresponsive to anti-PD-1/PD-L1 mAbs^{18, 19}. Thus, there remains a
85 critical need to identify and therapeutically modulate immune checkpoint pathways that function
86 independently of specific cell surface ligands.

87 The cytokine induced SH2 protein CISH is a recently identified cancer immune checkpoint that
88 functions as a negative modulator of TCR signaling and cancer neoantigen recognition. Unlike PD-1,
89 CISH is an intracellular protein that negatively regulates antigen-specific cytokine release and T cell
90 expansion via its capacity to bind PLC- γ 1, a proximal mediator of TCR complex signaling, for targeted
91 proteasomal degradation^{20, 21, 22, 23}. Germline deletion of *Cish* in mouse tumor-specific CD8⁺ T cells
92 promotes their expansion and cytokine polyfunctionality resulting in increased durable regression of
93 established melanoma lesions²². Ablation of *CISH* in human TIL cells increases antigen-specific T cell
94 proliferation, TCR functional avidity, and neoantigen reactivity²⁰. Additionally, CISH has recently been
95 shown to play an important role in negatively regulating Natural Killer (NK) cell persistence and *in vivo*
96 anti-tumor activity by suppressing activation downstream of the IL-15 receptor^{24, 25, 26}.

97 CISH is distinct from conventional cell surface immune checkpoint receptors. Unlike molecules
98 such as PD-1 and cytotoxic T-lymphocyte-associated protein 4 (CTLA-4) that operate by binding to
99 tumor cells ligands (PD-L1 and CD80 respectively), the CISH-PLC- γ 1 interaction occurs within the intra-
100 cellular compartment downstream of the TCR. Although inactivation of cell-surface immune
101 checkpoints may be achieved through mAb-based targeting, intra-cellular signaling molecules such as
102 CISH have historically remained unreachable (and thus undruggable). However, the advent of targeted
103 gene editing tools, such as CRISPR, now permit the precise, irreversible, and efficient inactivation of
104 CISH in human T cells²⁰. The potential of this novel immune checkpoint target to improve T cell
105 therapies for solid cancers is now being investigated in patients using CRISPR engineered CISH
106 knockout tumor infiltrating lymphocytes (TIL) ([NCT04426669](#)).²⁷

107 In a pre-clinical murine model, we recently demonstrated that CISH knockout results in
108 enhanced tumor regression when combined with PD-1 mAb blockade²⁰. In the present manuscript,
109 we now seek to understand the functional relationship between these two immune checkpoint targets
110 further. To test for potential synergy, we developed a highly efficient multiplex CRISPR editing
111 approach for use in primary human T cells. We targeted multiple immune checkpoint genes
112 simultaneously, allowing us to compare the CISH knockout phenotype with that of PD-1 and the
113 evolving cell surface immune checkpoint, T cell Immunoreceptor with Ig and ITIM domains (TIGIT).
114 Analysis of the effector function of immune checkpoint-deficient T cells showed that inactivation of
115 CISH leads to an enhanced program of T cell activation, memory formation, and antigen-specific
116 cancer cell cytotoxicity that individually is superior to, and in combination synergistic with, PD-1 and TIGIT
117 disruption. Importantly, the benefit of CISH disruption occurred independently of PD-L1 expression, a
118 finding that contrasts with the function of both PD-1 and TIGIT disruption. Together, our findings
119 demonstrate an important role for CISH in controlling T cell responses to cancer in a manner that is
120 independent of PD-L1/PD-L2 ligand expression. These results establish a unique and non-overlapping
121 role for CISH compared to canonical cell surface immune checkpoint targets such as PD-1/PD-L1.

122

123

124

125

126

127

128

129

130

131 RESULTS

132

133 *Multiplex gene editing enables the evaluation of CISH and other immune checkpoints in*
134 *regulating antigen-specific T cell function.*

135 To evaluate the immune function of CISH in relation to PD-1 and TIGIT in primary human T
136 cells, we developed a CRISPR/Cas9-based strategy for efficient multiplexed gene editing followed by
137 a functional evaluation using a real-time cancer cell cytolytic assay (**Fig. 1a**). We identified multiple
138 guide RNAs targeting the *CISH*, *PDCD1*, and *VSIG9* (the gene encoding TIGIT) loci that resulted in a
139 significant reduction in expression of the corresponding proteins (**Fig. 1b, c, & d**). A high level of
140 genetic knockout enabled us to assess the phenotypic and functional consequences of inactivating
141 these immune checkpoints in a head-to-head-to-head fashion. To measure T cell function, we
142 simultaneously introduced a double-strand break within the TCR alpha locus (*TRAC*) combined with
143 adeno-associated virus (AAV) delivery of a DNA repair template to introduce a previously described
144 recombinant TCR specific for the KRAS(G12D) shared cancer neoantigen²⁸. Integration of the
145 exogenous KRAS(G12D) TCR occurred at high frequency, as measured by expression of the murine
146 TCR β constant chain (mTCR β), while simultaneous CRISPR targeting of the *TRAC* locus removed
147 expression of the endogenous TCR (**Fig. 1e**). Transgenic TCR integration at the endogenous *TRAC* locus
148 afforded more robust TCR expression than targeting the *AAVS1* safe-harbor site. Stable levels of TCR
149 expression was observed over three-weeks of *ex vivo* T cell culture (**Fig. 1f**). Overall, this multiplex
150 CRISPR/AAV platform enabled the generation of a pool of edited T cells in which at least 50% have lost
151 expression of two immune checkpoint genes while simultaneously introducing an antigen-specific
152 TCR. This allowed a comparative investigation into the functional impact of immune checkpoint
153 modulation on human T cell biology.

154

155 *CISH inactivation enhances T cell activation, cytokine production and the formation of effector*
156 *memory cells.*

157 Given the intra-cellular nature of CISH and its capacity to attenuate proximal TCR signaling,
158 we hypothesized that disruption of CISH in naïve human T (T_N) cells derived from the peripheral blood
159 would result in an enhanced program of TCR-mediated effector functions. We first analyzed the
160 formation of distinct T cell memory subsets upon anti-CD3/CD28 stimulation of CD8⁺ T_N cells by
161 measuring expression of the memory markers CD45RA and CD45RO. We categorized the cell
162 populations as being either T_N /T stem cell memory (T_{SCM}) (CD45RO⁻, CD45RA⁺) or conventional
163 memory phenotype (CD45RO⁺, CD45RA⁻). CISH knockout T cells showed a significant increase in the
164 transition to a conventional memory T cell phenotype when compared to control T cells (**Fig. 2a**).

165 Further delineation of the T cell memory phenotype by analysis of the lymphoid-homing marker CD62L
166 within the CD45RO⁺ population revealed that CISH inactivation elevated the formation of an effector
167 memory T (T_{EM}) cell phenotype (CD62L⁻CD45RO⁺CD45RA⁻) (**Fig. 2a & b**).

168 Expression of the co-inhibitory PD-1 and TIGIT receptors was similar between control and CISH
169 knockout peripheral T cells (**Fig. 2c**). TCR stimulation alone was sufficient to reveal a stronger induction
170 of cytokine secretion by CISH knockout versus control T cells and a significant increase in IFN- γ and
171 TNF α expression (**Fig. 2d**) and increased cytokine polyfunctionality (**Fig. 2e & f**). No cytokine secretion
172 by CISH knockout T cells was observed in the absence of TCR stimulation. Taken together, these data
173 show that TCR stimulation of human CISH knockout T cells results in a significant elevation in the
174 formation of activated memory T cells with increased production of multiple cytokines.

175

176 *PD-1 or TIGIT knockout T cells fail to enhance T cell function following TCR stimulation.*

177 T cells deficient for either PD-1 or TIGIT showed no increase in the formation of T_{EM} cells in
178 response to anti-CD3/CD28 stimulation, in contrast with CISH KO cells (**Fig. 3a & b**). Furthermore, lack
179 of PD-1 or TIGIT also had no impact on the production of cytokines or cytokine polyfunctionality,
180 whereas CISH significantly elevated IFN- γ , TNF α , and the proportion of T cells expressing 2 or more
181 cytokines (**Fig. 3c & d**). As seen with CISH knockout T cells, lack of PD-1 did not increase expression of
182 TIGIT, and conversely lack of TIGIT did not increase expression of PD-1 (**Fig. 3e**). The lack of an increase
183 in functional response when PD-1 and TIGIT are deleted in T cells suggests that stimulation of the TCR
184 alone is insufficient to enhance T cell activation in the absence of expression for cell surface immune
185 checkpoints.

186

187 *CRISPR inactivation of CISH enhances antigen-specific T cell cytotoxicity of tumor cells.*

188 To resolve the impact of CISH disruption on neoantigen-specific tumor cytotoxicity, we developed
189 a real-time kinetic cancer cell cytotoxicity assay using an automated xCELLigence Real-Time Cell Analysis
190 (RTCA) instrument. By co-culturing T cells expressing the KRAS(G12D)-specific TCR with HLA-C*08:02⁺
191 cells pulsed with either the KRAS(G12D) minimal epitope or the corresponding wild type (WT)
192 sequence, we could reveal an effective level of antigen-specific killing, defining a robust assay window
193 to measure the impact of immune checkpoint gene inactivation on antigen-specific cytotoxicity (**Fig. 4a**).
194 Killing of antigen-bearing cells by CISH-deficient, KRAS(G12D) TCR expressing CD8⁺ T cells was
195 significantly elevated, both in rapidity and in overall magnitude of response, at timepoints throughout
196 the 5-day co-culture (**Fig. 4b and c**). Co-incubation of CRISPR edited CD8⁺ T cells with the antigen-
197 bearing target cells also lead to a measurable antigen-specific cell lysis at 16 and 48 hours when
198 measured by an orthogonal assay utilizing apoptosis-specific dyes, which was significantly increased

199 by inactivation of CISH (**Fig. 4d**). These cytolytic data demonstrate that inactivation of CISH
200 significantly elevates the neoantigen-specific killing of target cells.

201

202 *The enhancement in T Cell function by PD-1 inactivation is only revealed in the presence of PD-*
203 *L1.*

204 We next sought to compare the enhanced cytotoxicity seen with CISH knockout to T cells lacking
205 PD-1 in the neoantigen-specific killing assay. Surprisingly, we did not observe any change in the killing
206 capacity of PD-1-deficient T cells towards the neoantigen expressing target cells when compared to
207 control cells at any effector to target ratio tested (**Fig. 4e**). When PD-1 knockout was combined with
208 CISH knockout in the same T cell pool, no additional benefit to PD-1 inactivation was seen above the
209 elevated cytotoxicity due to CISH-deficiency alone (**Fig. 4e**). These data suggested that unlike T cells
210 lacking CISH, these conditions of neoantigen-specific TCR stimulation were insufficient for PD-1
211 disruption to benefit the cytolytic response.

212 We reasoned that absence of increased cytotoxicity when PD-1 is knocked out could be due to a
213 requirement for PD-L1 ligand. COS-7 is a monkey kidney fibroblast cell line that does not express high
214 levels of PD-L1; thus, PD-1 knockout T cells were unlikely to have an advantage in eliciting a stronger
215 cytolytic response^{29, 30}. To test the requirement for PD-L1, we selected MM.1S, a multiple myeloma
216 cell line that expresses high levels of PD-L1^{31, 32} (**Fig. 4f**). When CISH knockout CD8⁺ T cells were co-
217 cultured with MM.1S cells for 16 hours, we observed a significantly elevated level of cytotoxicity
218 compared with control T cells. Similarly, we observed that T cells deficient for PD-1 also exhibited
219 increased cytotoxicity, albeit at a lower magnitude compared with CISH-deficient T cells (**Fig. 4g**). These
220 data confirmed that PD-1 editing only leads to enhanced cytotoxicity when PD-L1 is expressed by a tumor
221 cell line. By contrast, CISH inactivation enhances the cytolytic activity of CD8⁺ T cells regardless of
222 immune checkpoint ligand expression.

223

224 *T cell cytotoxicity of PD-L1 expressing tumor cells is enhanced by PD-1 knockout and further*
225 *elevated in CISH-deficient T cells.*

226 We next analyzed cytotoxicity of a high PD-L1 expressing cancer cell line by immune checkpoint
227 knockout T cells. Expression of PD-L1 in different tumor lines was analyzed and the ES-2 ovarian clear
228 cell carcinoma line was selected based on its highest expression of PD-L1 (**Fig. 5a**). This cell line is WT
229 KRAS but expresses the HLA-C*08:02 allele, as confirmed by MHC allele sequencing and from
230 published HLA haplotype data (**Supplementary Fig. S1**)^{33, 34, 35, 36}. Thus, in addition to expressing high
231 levels of PD-L1, the ES-2 cell line can be used to present the HLA-C*08:02 restricted KRAS(G12D)
232 peptide to the recombinant TCR expressing T cells when pulsed onto the cell line. To compare the

233 requirement of PD-1 signaling in T cell cytolysis within the same cell type, CRISPR was used to knockout
234 the PD-L1 and PD-1 ligand 2 (PD-L2) genes in the ES-2 line (**Fig. 5b**). PD-L2 is expressed on antigen-
235 presenting cells and certain tumors, including ovarian cancers. Like PD-L1, PD-L2 has also been shown
236 to bind PD-1 and inhibit TCR-mediated proliferation and cytokine production³⁷. We first analyzed the
237 cytolysis of ES-2 cells by control CD8⁺ T cells expressing the KRAS(G12D) TCR and observed antigen-
238 specific killing of cells presenting the KRAS(G12D) neoantigen. (**Fig. 5c**). CISH-deficient T cells showed
239 a significant increase in antigen-specific cytolysis over control T cells of both the parental ES-2 and the
240 PD-L1/PD-L2 knockout cells (**Fig. 5c & d**). While cytolysis of the high PD-L1/PD-L2 ES-2 cells by PD-1
241 knockout T cells showed an increase over control T cells, PD-1 knockout T cells did not elevate the
242 overall killing of PD-L1/PD-L2 deficient ES-2 cells (**Fig. 5e & f**). Despite enhancing cytolysis of the PD-
243 L1/PD-L2 expressing cancer cells over control T cells, editing of PD-1 was less effective than CISH
244 inactivation.

245 Analysis of ES-2 cell cytolysis by TIGIT knockout T cells revealed a similar pattern to that seen
246 by inactivation of PD-1, with TIGIT-deficient T cells enhancing cytolysis of ES-2 parental cells
247 significantly over control T cells and a lack of improvement in killing of ES-2 cells lacking PD-L1/PD-L2
248 (**Fig. 5g & h**). The dependency of PD-L1/PD-L2 expression on TIGIT regulation of cytolysis may not be
249 surprising, as recent evidence suggests T cell functional and anti-tumor responses regulated by TIGIT
250 and PD-1 appear to be overlapping and co-dependent^{38, 39}. Despite significantly elevated cytolysis by
251 TIGIT knockout T cells over control, CISH-deficient T cells lead to the highest increase in antigen-
252 specific cytolysis of these ovarian cancer cells (**Fig. 5g & h**). Collectively, these data indicate an
253 essential requirement for PD-L1 expression by cancer cells for any demonstrable effect on anti-tumor
254 responses by PD-1 knockout and TIGIT knockout T cells. By contrast, CISH inactivation showed superior
255 improvements in cytolysis irrespective of PD-L1/PD-L2 expression.

256

257 *Enhanced anti-tumor cytolysis by CISH-deficient T cells is synergistic in combination to PD-1 or*
258 *TIGIT immune checkpoint knockout.*

259 Finally, given the ligand restriction of PD-1 signaling and expected distinct and non-redundant
260 role with CISH-mediated abrogation of proximal TCR signaling, we evaluated the potential synergy of
261 PD-1 and CISH knockout in the context of neoantigen-specific cancer cell killing. To this end, we
262 performed multiplex CRISPR engineering in KRAS(G12D) TCR targeted CD8⁺ T cells to knockout CISH in
263 combination with either PD-1 or TIGIT in the same pool of T cells and analyzed cytolysis of the ES-2
264 parental and ES-2 PD-L1/PD-L2 knockout cancer cells. Combined inactivation of CISH and PD-1 resulted
265 in a significantly elevated killing of the parental ES-2 cell lines above either immune checkpoint alone
266 at all timepoints measured (**Fig. 6a**). This combined efficacy was only evident when PD-L1/2 ligands

267 were present, as the CISH plus PD-1 knockout T cells showed no further increase in killing of ES-2 cells
268 lacking PD-L1/PD-L2 above CISH knockout alone.

269 Like PD-1, knockout of TIGIT in combination with CISH inactivation also showed an enhanced
270 level of neoantigen-specific cytolysis of the PD-L1/PD-L2 expressing cancer cells (**Fig. 6a**). Again,
271 improved killing was only evident in the presence of PD-L1/PD-L2, further demonstrating that cell
272 surface immune checkpoints such as PD-L1 and TIGIT can only add additional cytolytic efficacy to CISH-
273 deficient T cells in a context where tumor cells express their ligands.

274

275

276

277

278

279

280

281

282

283

284

285

286

287

288

289

290

291

292

293

294

295

296

297

298

299

300

301 DISCUSSION

302

303 Tumor resident antigen-specific T cells, such as neoantigen reactive TIL, can recognize and clear cancer
304 cells, although the clinical efficacy remains promising yet inconsistent with or without combined
305 immune checkpoint inhibition^{40, 41}. The TME exerts complex and mostly understudied mechanisms
306 for suppressing T cell function and the upregulation of cell surface immune checkpoint proteins,
307 reduced MHC expression on cancer cells, and low antigen density are only some of the main extrinsic
308 factors contributing to a weakened and short-lived cytolytic T cell response after TCR activation^{42, 43,}
309 ⁴⁴.

310 MAb-based therapies for inactivating classical cell-surface immune checkpoints such as PD-
311 1/PD-L1, CTLA-4, and possibly TIGIT can help to overcome some of the suppressive effects of the TME
312 on cancer neoantigen-specific T cells and have shown promising clinical outcomes in a subset of
313 patients⁴⁵. However, the requirement for the cancer to express high levels of PD-L1 for mAb blockade
314 to have any meaningful clinical efficacy, and the heterogeneity in PD-L1 expression between cancer
315 types and individuals, restricts the efficacy of this therapeutic approach to a relatively restricted
316 subset of responsive patients⁴⁶.

317 A new class of intra-cellular immune checkpoints, exemplified by CISH, have the potential to
318 overcome this limit of ligand-dependency and have the potential to enhance the anti-tumor functions
319 of T cells against any cancer in a PD-L1 agnostic manner. Recent studies have highlighted that CISH is
320 highly expressed in activated T cells and TILs isolated from patient tumors and demonstrate the
321 important role CISH plays in negatively regulating TCR avidity, tumor cytolysis and neoantigen
322 recognition^{20, 22, 23}. Furthermore, the inactivation of CISH in human TIL resulted in improved antigen-
323 specific activation and unmasked reactivity against shared neoantigens, suggesting that ablation of
324 CISH within the TME may help cancer-specific T cells to overcome T cell intrinsic suppression of the
325 cytolytic response and augment the anti-cancer activity of these reactive cells. The additional finding
326 of increased PD-1 expression in CISH-deficient T cells, and a synergistic response of combined CISH
327 and PD-1 inactivation in a murine melanoma model, warranted further investigation of the
328 comparison and combination of these non-redundant immune checkpoint pathways²⁰.

329 In the current study we build upon recent findings that demonstrate the role of CISH in
330 modulating T cell anti-tumor functions, neoantigen reactivity, and cytolytic effector programs by
331 evaluating the impact of CISH inactivation in antigen-specific, anti-tumor T cell functions in
332 comparison and combination to PD-1 and TIGIT. We developed an optimized CRISPR/Cas9 editing
333 strategy that enables efficient simultaneous genetic disruption of multiple immune checkpoint genes

334 in human T cells while concurrently targeting the endogenous TCR locus to stably integrate and
335 express a recombinant TCR specific to the human shared neoantigen, KRAS(G12D).

336 Our findings demonstrate that CISH knockout results in a significant enhancement in TCR
337 stimulated T_{EM} cell formation and cytokine production, highlighting the important role this target plays
338 downstream of the activated TCR. Surprisingly, our experiments did not show a similar significant
339 enhancement of these functional T cell responses when either PD-1 or TIGIT was inactivated by
340 CRISPR. This finding suggests that unlike CISH, TCR stimulation alone may not be sufficient to reveal
341 the benefits of disruption of PD-1 and TIGIT signaling pathways in T cells.

342 To accurately compare the impact of genetic disruption of immune checkpoint genes on anti-
343 tumor activity *in vitro*, we developed an evaluation platform where CRISPR-edited T cells can be tested
344 for their capacity to kill neoantigen-bearing tumor cells in a sensitive and real-time assay. These tumor
345 cell killing assays demonstrated that cytolysis of antigen-expressing tumor cells by CISH-deficient T
346 cells was significantly elevated over control T cells. Furthermore, the finding that CISH knockout led
347 to elevated tumor cell killing in all conditions and biological donors tested, regardless of the cell type
348 or PD-L1 expression, supports the notion that CISH, by virtue of being intra-cellular and a key regulator
349 of proximal TCR signaling, operates to control T cell responses in a ligand-independent manner.
350 Antigen-specific TCR stimulation alone was not sufficient for PD-1 inactivation to benefit anti-tumor
351 responses. Further, we demonstrated that expression of PD-L1/L2 is required for PD-1 knockout T cells
352 to enhance cytolysis.

353 Interest in TIGIT as an anti-cancer target has increased recently and anti-TIGIT mAbs are now
354 being evaluated in early clinical trials with modest yet evolving data^{47, 48}. While more is known
355 regarding the biology of PD-1 and its ligand interactions, ligands of TIGIT have been identified as
356 poliovirus receptor (PVR), Nectin2, Nectin3 and Nectin4 and have been shown to be expressed by
357 tumor cells and antigen-presenting cells within the TME^{49, 50, 51, 52}. Our data showing TIGIT-deficient T
358 cells induced a similar cytolytic response to PD-1 knockout T cells, whereby an enhanced level of tumor
359 cell killing was revealed in the absence of PD-L1 signaling, suggests a potential interdependency on
360 PD-1-mediated inhibition of T cell activation and function.

361 The precision and efficiency of multiplex CRISPR editing enables the inactivation of multiple
362 genes within the same T cell and enables us to evaluate the combined genetic disruption of both CISH
363 and PD-1 or TIGIT. The enhancement of neoantigen-specific tumor cell killing that we observed
364 suggests that CISH and PD-1 independently regulate T cell function using non-redundant signaling
365 pathways. These findings highlight the promising notion of combination immune checkpoint inhibition
366 for enhancing anti-cancer response that may leverage the distinct pathways of both intra-cellular and
367 cell surface immune checkpoint targets. As predicted, this additive response was only seen against

368 tumor cells expressing high levels of PD-L1, whereby PD-1 knockout or TIGIT knockout appears to
369 bypass the suppressive effects of PD-L1 expression and enhance cytotoxicity above and beyond the
370 increased killing observed with CISH-inactivation alone.

371 The ideal attributes of immune checkpoint targets for efficacy in solid cancers can be
372 considered in terms of the effectiveness of tumor cell killing and accessibility for precise drugging and
373 thus therapeutic inhibition. As summarized in **Table 1**, these attributes show distinct differences
374 between cell surface immune checkpoints PD-1 and TIGIT, and the intra-cellular immune checkpoint
375 CISH. While disruption of all these targets can improve neoantigen-specific tumor cell lysis as
376 demonstrated in this study, the ligand independency of CISH offers the potential for broadening
377 immune checkpoint therapies against any solid cancer. The durable clinical benefit of anti-PD-1
378 immunotherapy is now well established and recent data suggests anti-tumor efficacy is also
379 achievable through TIGIT blockade in combination to anti-PD-L1 therapy⁴⁷. The intra-cellular nature
380 of CISH makes conventional immune checkpoint inhibition using a mAb-based therapy challenging.
381 While direct intra-cellular protein drugging modalities for CISH may one day be possible, precision
382 genetic engineering has now enabled the efficacy of the CISH immune checkpoint to be objectively
383 evaluated in ongoing clinical trials.

384 The finding that concurrent inactivation of CISH and PD-1 can act together to further improve
385 the tumor-specific cytolytic potential of T cells offers a compelling prospect for a dual-therapeutic
386 approach to target both immune checkpoint genes in a hope to engender a T cell therapy with a
387 durable and complete anti-cancer response. The enhanced anti-tumor response observed with CISH-
388 deficient T cells in this and other published reports positions CISH as a next-generation intra-cellular
389 immune checkpoint target that may have meaningful clinical efficacy in the setting of a broad cross-
390 section of solid cancers, irrespective of the presence of PD-L1/PD-L2 or other immunosuppressive
391 ligands.

392

393

394

395

396

397

398

399

400

401

402 **METHODS**

403

404 *PBMC samples and isolation of CD8⁺ T cells*

405 Peripheral blood mononuclear cells were obtained from anonymized healthy individuals (Caltag
406 Medsystems, Tissue Solutions Ltd and Precision for Medicine, Inc.) and obtained, handled, and stored
407 in accordance with the Human Tissue Authority UK regulations. Total CD8⁺ T cells were isolated from
408 unfractionated PBMCs using the EasySep Human CD8⁺ T Cell Isolation Kit (Stem Cell Technologies) with
409 a DynaMag-2 magnet (ThermoFisher Scientific) according to the manufacturer's guidelines. The ratio
410 of CD8:CD4 and viability of isolated T cells was assessed regularly using flow cytometry.

411

412 *Expansion of CD8⁺ T cells*

413 Isolated human CD8⁺ T cells were cultured in X-VIVO-15 Basal Media (Lonza) supplemented with 10%
414 Human AB Serum Heat Inactivated (Sigma), 300IU/ml Recombinant Human IL-2, 5ng/ml Recombinant
415 Human IL-7, and 5ng/ml Recombinant Human IL-15 (all Peprotech) and 10mM N-Acetyl-L-cysteine
416 (Sigma) and cultured in a 37°C, 5% CO₂ cell culture incubator. Media was replaced every 2-3 days with
417 fresh complete media including cytokines.

418

419 *Cell Lines and Culturing*

420 All cell lines used for this study were purchased from ATCC and cultured in their recommended media
421 formulations and growth conditions. Cells were kept at sub-confluent densities and regularly tested
422 for mycoplasma. SV40-transformed COS-7 cells were engineered to express a human HLA C*08:02
423 allele to enable presentation of pulsed KRAS wildtype and mutant peptides. HLA-A/B/C allele typing
424 for each cell line was performed by MC Diagnostics Ltd (UK).

425

426 *sgRNA Design*

427 sgRNAs targeting *TRAC*, *CISH*, *PDCD1*, *VSIG9*, *PDCD1LG1* (*PD-L1*), and *PDCD1LG2* (*PD-L2*) were
428 designed using various online resources. Up to 6 sgRNAs per target gene were tested and the most
429 efficient sgRNA was selected containing 2'-O-methyl and 3' phosphorothioate modifications to the
430 first three 5' and the last three 3' nucleotides (Synthego).

431

432 *Production of AAV-mediated TCR-Knock-in and checkpoint-knockout CD8⁺ T cells using* 433 *CRISPR/Cas9*

434 CD8⁺T cells were stimulated using anti-CD3/CD28 Dynabeads (Life Technologies) in complete T cell
435 media and under normal growth conditions for 48-72 hours prior to electroporation. T cells were

436 electroporated in Neon Buffer T with 15 μ g Cas9 mRNA (TriLink) and 10 μ g total sgRNA (Synthego) using
437 the Neon electroporator (3x10⁶ cells per 100 μ l tip) (Life Technologies) using parameters 1400V, 10ms,
438 3 pulses. To achieve targeted recombinant TCR integration into the *TRAC* locus, rAAV6 was added to
439 CD8⁺ T cells 3-5 hours after electroporation at an MOI of 1x10⁶ particles per cell. Viral rAAV6 particles
440 were produced by Vigene Biosciences or PackGene. Electroporated T cells were recovered in complete
441 T cell media at a density of 1x10⁶ cells per ml and allowed to rest for 48 hours before subsequent
442 analysis.

443

444 *Analysis of Gene Knockout Efficiency on DNA Level*

445 Primers for PCR were designed to amplify a 600-900 base pair region surrounding the sgRNA target
446 site. A minimum of 24 hours after electroporation, genomic DNA was extracted from CD8⁺ T cells using
447 the DirectPCR Lysis solution (Viagen Biotech) containing Proteinase K and target regions were
448 amplified by PCR using the GoTaq G2 PCR mastermix (Promega). Correct and unique amplification of
449 the target regions was verified by agarose gel electrophoresis before purifying PCR products using the
450 QIAquick PCR Purification Kit (Qiagen). For analysis by TIDE, PCR amplicons were Sanger sequenced
451 (Eurofins or Genewiz), and paired .ab1 files of control versus edited samples were analyzed using
452 Synthego's ICE tool (<https://ice.synthego.com>).

453

454 *Immunoblot analysis*

455 *Western* blot analysis was performed using standard protocols. In brief, cells were harvested and
456 washed once in ice-cold PBS and then lysed in 1X RIPA Buffer containing 1X Protease Inhibitors on ice
457 for 10 minutes. Cells were then centrifuged in a table-top centrifuge at 14,000 rcf for 20 min at 4°C to
458 pellet cell debris. Proteins were separated on a 4–12% SDS-PAGE gel followed by standard
459 immunoblot analysis using anti-CISH (Cell Signaling, Clone D4C10, 1:2000) and Vinculin (Cell Signaling,
460 Clone EPR8185, 1:5000). Detection of proteins was performed using secondary antibodies conjugated
461 to horseradish peroxidase-HRP and the SuperSignal West Pico Plus chemiluminescent substrate
462 (Thermo Scientific-Pierce).

463

464 *Flow cytometry analysis of T cell phenotypes*

465 For flow cytometric analysis of the CRISPR edited T cell phenotypes and cell surface marker
466 expression, cells were harvested from culture plates and washed using FACS Buffer containing PBS
467 with 0.5% Bovine Serum Albumin (Thermo Scientific) and were then stained with monoclonal
468 antibodies specific for CD8 (HIT8A, 1:100), CD4 (OKT4, 1:100), HLA-DR (L243 1:80), LAG-3 (11C3C65,
469 1:80), TIGIT (VSTM3, 1:40), CD45RO (UCHL1, 1:40), CD45RA (HI100, 1:80), TIM3 (F38-2E2, 1:40), CD62L

470 (DREG-56, 1:40), CD57 (QA17A04, 1:80), PD-1 (EH12.1, 1:40), OX-40 (Ber-ACT35, 1:40), CD25 (MA2-
471 51, 1:40), 41BB (4B4-1, 1:40), (Biolegend) or specific for CD8 (RPA-T8, 1:100) (BD Bioscience) and CD3
472 (UCHT1, 1:100) (ThermoFisher). Live/Dead Fixable Dead Cell Stains (Invitrogen) or SYTOX Blue Dead
473 Cell Stain (Invitrogen) were included in all experiments to exclude dead cells. All samples were
474 acquired on a Fortessa flow cytometer (BD Bioscience), and data was analyzed using FlowJo 10
475 software (BD Biosciences).

476

477 *Intra-cellular cytokine staining*

478 Cells were stimulated for a total of 6 hours with human T-activator anti-CD3/CD28 Dynabeads
479 (ThermoFisher) stimulation with GolgiStop solution being added for a total of 5 hours block intra-
480 cellular protein transport (BD Bioscience). As a positive control for cytokine production, a pool of T
481 cells was stimulated for 6 hours with 50ng/ml PMA and 1 μ g/ml Ionomycin (Sigma). T cells were then
482 harvested and washed with FACS Buffer and stained for surface markers followed by fixation and
483 permeabilization using BD Cytofix/Cytoperm Fixation/Permeabilization Solution (ThermoFisher)
484 before proceeding with intra-cellular cytokine staining using antibodies specific for INF- γ (4S.B3, 1:40)
485 (Biolegend) IL-2 (MQ1-17H12, 1:40) (BD Bioscience), or TNF- α (MAb11, 1:40) (ThermoFisher). All
486 samples were acquired on a Fortessa flow cytometer (BD Bioscience), and data was analyzed using
487 FlowJo 10 software (BD Biosciences).

488

489 *Realtime Cytolysis Assay (RTCA)*

490 Cytolysis assays were carried out with the xCELLigence RTCA SP platform (Acea Bioscience/Agilent)
491 based on electrical impedance resulting in a cell index (CI) value. Background measurements were
492 taken with media only before seeding cells. Adherent COS-7 or ES-2 tumor cells were then plated in a
493 96-well RTCA View plate at a pre-determined density per well to reach a linear growth time phase
494 after roughly 14-18 hours of culture and incubated overnight at 37°C and 5% CO₂ in their respective
495 complete growth medium. The next day, cancer cells were pulsed with mutant (G12D) or wildtype
496 (WT) peptides for 2 hours and then washed prior to the addition of different knockout T cells or
497 Control T cells. T cells were added at indicated effector to target cell ratios (E:T) and containing the
498 respective gene edits. Cytolysis assays were run for up to 90 hours undisturbed with measurements
499 taken every 2-10 minutes. Data was analyzed using RTCA software and plotted as % Cytolysis
500 calculated as (impedance of target cells without effector cells – impedance of target cells with effector
501 cells) x100 divided by impedance of target cells without effector cells. Controls include background
502 measurements as well as a negative control containing target cells only as well as a positive control
503 containing target cells receiving 2.5% Triton-x solution for maximum cytolysis.

504

505 *Statistical analyses*

506 Statistical differences between two sample groups, where appropriate, were analyzed by a standard
507 Student's two-tailed, non-paired, t-test and between three or more sample groups using two-way or
508 three-way ANOVA using GraphPad Prism Software version 9. P values are included in the figures where
509 statistical analyses have been carried out.

510

511 **Ethics declarations**

512

513 The authors declare no competing interests.

514

515 **ACKNOWLEDGEMENTS:**

516

517 This study was supported by Intima Bioscience, NIH R37 CA259177 (C.A.K.), and NIH P30 CA008748
518 (C.A.K.).

519

520

521

522

523

524

525

526

527

528

529

530

531

532

533

534

535

536

537

538 **FIGURES**

539

540 **Figure 1: Multiplex CRISPR/rAAV editing of *CISH* and *KRAS(G12D)* TCR integration in primary human**

541 **T cells. (a)** Schematic diagram of a multiplex CRISPR/rAAV genome engineering and cancer cell

542 cytotoxicity assay platform for primary human CD8⁺ T cells. **(b)** Efficient disruption of the intra-cellular

543 checkpoint gene *CISH* measured on DNA level by Sanger sequencing and reduced *CISH* protein

544 expression measured by Western blot. **(c)** T cell surface expression of immune checkpoint genes PD-

545 1 and TIGIT measured by flow cytometry with or without multiplex CRISPR editing. **(d)** The frequency

546 of CD8⁺ T cells with disrupted immune checkpoint genes after simultaneous multiplex editing. **(e)**

547 Targeting of the *TRAC* locus for rAAV-mediated insertion of the recombinant *KRAS(G12D)*-specific TCR

548 results in loss of endogenous TCR expression while enabling high expression of the exogenously

549 introduced TCR. **(f)** Comparison of recombinant TCR expression over 3 weeks following CRISPR/rAAV

550 engineering of primary human CD8⁺ T cells when integrated into either the *TRAC* or *AAVS1* locus.

551 Statistical significance was determined by either student t test or ANOVA for repeated measures; *P

552 <0.05, **P<0.01, ***P<0.001, ****P<0.0001. All data are representative of at least three independent

553 experiments. Error bars represent mean +/- SEM.

554

555 **Figure 2: Inactivation of *CISH* in human T cells enhances T cell effector function upon TCR signaling.**

556 **(a)** Knockout (KO) of *CISH* in CD8⁺ T cells increases the proportion of cells with a memory phenotype

557 upon anti-CD3/CD8 stimulation (upper panels) and the effector memory proportion T_{EM} (lower

558 panels). **(b)** Quantification of changes in memory phenotypes in CD8⁺ T cells in control and *CISH*-

559 knockout as in (a). **(c)** Expression of inhibitory receptors PD-1 and TIGIT is similar between *CISH* KO

560 and control T cells. **(d-e)** Knockout of *CISH* in CD8⁺ T cells significantly increases the magnitude of

561 effector cytokine production and the frequency of T cells expressing 2 or 3 cytokines as measured by

562 intra-cellular cytokine staining (ICS). **(f)** *CISH* knockout in CD8⁺ T cells increases the total number of

563 polyfunctional CD8⁺ T cells after TCR stimulation via anti-CD3/CD28 beads. In addition, *CISH* knockout

564 elevates the ratio of T cells expressing 1:2:3 cytokines. For polycytokine visualization one

565 representative donor is shown. Statistical significance was determined by either student t test or

566 ANOVA for repeated measures, *P >0.05, **P>0.01, ***P>0.001, ****P>0.0001. All data are

567 representative of at least three independent experiments. Error bars represent mean +/- SEM.

568

569 **Figure 3: PD-1 or TIGIT disruption does not enhance in T cell effector functions upon TCR signaling.**

570 **(a)** The increase in T cell memory formation measured by flow cytometry after anti-CD3/CD8

571 stimulation, in particular effector memory cells, observed by knockout of *CISH* is not seen by either

572 PD-1 or TIGIT inactivation. **(b)** Quantification of changes in memory phenotypes in CD8⁺ T cells in
573 control or inactivation of CISH, PD-1, or TIGIT. **(c)** Knockout of CISH significantly increases the
574 magnitude of effector cytokine production measured by ICS after anti-CD3/CD8 stimulation, whereas
575 PD-1 or TIGIT knockout results in cytokine production similar to control T cells. **(d)** Contrary to CISH
576 knockout CD8⁺ T cells, PD-1 or TIGIT knockout does not enhance cytokine polyfunctionality. **(e)**
577 knockout of PD-1 has no impact on expression of TIGIT in anti-CD3/CD8 stimulated CD8⁺ T cells, and
578 similarly knockout of TIGIT does not impact expression of PD-1. Statistical significance was
579 determined by either student t test or ANOVA for repeated measures, *P >0.05, **P>0.01,
580 ***P>0.001, ****P>0.0001. All data are representative of three independent experiments. Error bars
581 represent mean +/- SEM.

582

583 **Figure 4: The increased antigen-specific cancer cell killing by CISH disrupted T cells is elevated above**
584 **that seen by PD-1 deficient T cells. (a)** A kinetic tumor impedance assay using the xCELLigence system
585 enables real-time measurement of KRAS G12D antigen-specific killing of peptide-pulsed COS-7 cell by
586 CRISPR edited CD8⁺ T cells. **(b)** Increase in the magnitude of antigen-specific cell cytolysis of antigen
587 pulsed COS-7 target cells in the absence of CISH. **(c)** Quantification of 16h, 48h, and 72h timepoints
588 from the cytolysis assay shows a significantly higher cytolytic response is observed at all timepoints
589 for CD8⁺ T cells lacking CISH compared to Control. **(d)** Similar results were observed in an orthogonal
590 assay for cytolysis using Cytox Green as an indicator for cell death when coculturing peptide pulsed
591 COS-7 target cells with control and CISH-edited CD8⁺ T cells, in the presence of cancer-specific KRAS
592 G12D antigen. **(e)** CISH inactivation enhances antigen-specific cytolysis compared to control T cells
593 and loss of PD-1 shows no improvement in cytolysis of COS-7 cells naturally lacking PD-L1. Targeting
594 both CISH and PD-1 shows no synergistic effect, emphasizing the ligand-dependency of PD-1 and
595 ligand independency of CISH in this cellular model. Control condition reflects the KRAS G12D TCR
596 knock-in only. Successful integration of the KRAS G12D TCR in these different gene-edited conditions
597 as well as knockout of the endogenous TCR is confirmed by flow cytometry (panels below). **(f)** The
598 myeloma MM.1S cell line shows a detectible PD-L1 expression which is robustly increased in response
599 to INF- γ stimulation. **(g)** When coculturing gene-edited CD8⁺ T cells with MM.1S cancer cells for 16
600 hours, both CISH knockout and PD-1 knockout T cell enhance the proportion of apoptotic MM.1S cells
601 (measure by Annexin-V staining) compared to control T cells. Statistical significance was determined
602 by either student t test or ANOVA for repeated measures, *P >0.05, **P>0.01, ***P>0.001,
603 ****P>0.0001. All data are representative of at least three independent experiments. Error bars
604 represent mean +/- SEM.

605

606 **Figure 5: Enhanced antigen-specific cytotoxicity of PD-1 and TIGIT-deficient T cells is dependent on PD-**
607 **L1 expression on the cancer cells, whereas elevated cytotoxicity by CISH inactivation is ligand-**
608 **independent. (a)** Human cancer cell lines exhibit varying expression of functional PDL-1 and PDL-2
609 receptors as shown by upregulation upon treatment with INF- γ for 48 hours. Human cancer cell lines
610 evaluated include ES-2 (yellow), BxPC-3 (orange), HCT-116 (red), SCC-25 (blue), MCF-7 (green),
611 OVCA9 (pink), and SW620 (purple). **(b)** Sequenced haplotype of HLA-C alleles for each cell line
612 evaluated. **(c)** Loss of expression of PD-L1 and PD-L2 on ES-2 cells engineered by CRISPR. **(d)** CISH
613 disruption enhances antigen-specific T cell cytotoxicity of KRAS G12D antigen-pulsed ES-2 human cancer
614 cells. **(e)** The same enhanced cytotoxicity by CISH inactivation is observed against the PD-L1/PD-L2
615 knockout ES-2 cells. **(f)** PD-1 knockout results in an increase in antigen-specific ES-2 cell cytotoxicity, **(g)**
616 but no significant overall increase in cytotoxicity towards the PD-L1/PD-L2 knockout ES-2 cells, indicating
617 a requirement for the ligands to be present to reveal a cytotoxic benefit for PD-1 inactivation. The
618 elevated cytotoxicity of ES-2 cells by PD-1 KO T cells is lower than observed with CISH KO T cells. **(h-i)**
619 Similar results are observed with TIGIT deficiency in CD8⁺ T cells improving cytotoxicity in the setting of
620 PD-L1/PD-L2 expression but showing no benefit when these ligands are absent on the ES-2 cells.
621 Antigen-specific cytotoxicity is elevated by T cells lacking CISH over TIGIT regardless of PD-L1/PD-L2
622 expression on the cancer cells. Statistical significance was determined by either student t test or
623 ANOVA for repeated measures, *P >0.05, **P>0.01, ***P>0.001, ****P>0.0001. All data are
624 representative of at least three independent experiments. Error bars represent mean +/- SEM.

625

626 **Figure 6: Inactivation of CISH and PD-1/TIGIT synergize to maximize the increase in antigen-specific**
627 **cancer cell cytotoxicity. (a)** Disruption of CISH in combination with PD-1 or TIGIT knockout both show
628 maximum and synergistic levels of antigen-specific cytotoxicity towards the high PD-L1/PD-L2 ES-2
629 myeloma cells. This synergy is only observed toward cancer cells harboring functional PD-L1 and PD-
630 L2 and not CRISPR engineered cells lacking these two ligands, emphasizing the ligand-dependency of
631 PD-1 (and TIGIT) and superior, ligand independency of CISH in this cellular model. Statistical
632 significance was determined by either student t test or ANOVA for repeated measures, *P >0.05,
633 **P>0.01, ***P>0.001, ****P>0.0001. All data are representative of at least three independent
634 experiments. Error bars represent mean +/- SEM.

635

636 **Table 1: The attributes of intra-cellular CISH inhibition in human T cells in comparison to cell surface**
637 **immune checkpoints PD-1 and TIGIT.**

638

639 **Supplementary Figure S1: Sequenced haplotype of HLA-C alleles for each cancer cell line evaluated.**

640 **REFERENCES**

641

642 1. Heslop, H.E. *et al.* Long-term restoration of immunity against Epstein-Barr virus infection by
643 adoptive transfer of gene-modified virus-specific T lymphocytes. *Nat Med* **2**, 551-555 (1996).

644

645 2. Campillo-Davo, D., Flumens, D. & Lion, E. The Quest for the Best: How TCR Affinity, Avidity,
646 and Functional Avidity Affect TCR-Engineered T-Cell Antitumor Responses. *Cells* **9** (2020).

647

648 3. Chandran, S.S. & Klebanoff, C.A. T cell receptor-based cancer immunotherapy: Emerging
649 efficacy and pathways of resistance. *Immunol Rev* **290**, 127-147 (2019).

650

651 4. Darvin, P., Toor, S.M., Sasidharan Nair, V. & Elkord, E. Immune checkpoint inhibitors: recent
652 progress and potential biomarkers. *Exp Mol Med* **50**, 1-11 (2018).

653

654 5. Song, M., Chen, X., Wang, L. & Zhang, Y. Future of anti-PD-1/PD-L1 applications:
655 Combinations with other therapeutic regimens. *Chin J Cancer Res* **30**, 157-172 (2018).

656

657 6. Munhoz, R.R. & Postow, M.A. Clinical Development of PD-1 in Advanced Melanoma. *Cancer J*
658 **24**, 7-14 (2018).

659

660 7. Rotte, A. Combination of CTLA-4 and PD-1 blockers for treatment of cancer. *J Exp Clin Cancer*
661 *Res* **38**, 255 (2019).

662

663 8. Sun, L. *et al.* Clinical efficacy and safety of anti-PD-1/PD-L1 inhibitors for the treatment of
664 advanced or metastatic cancer: a systematic review and meta-analysis. *Sci Rep* **10**, 2083
665 (2020).

666

667 9. Upadhaya, S. *et al.* Combinations take centre stage in PD-1/PDL1 inhibitor clinical trials. *Nat*
668 *Rev Drug Discov* (2020).

669

670 10. Seidel, J.A., Otsuka, A. & Kabashima, K. Anti-PD-1 and Anti-CTLA-4 Therapies in Cancer:
671 Mechanisms of Action, Efficacy, and Limitations. *Front Oncol* **8**, 86 (2018).

672

673 11. Riley, J.L. PD-1 signaling in primary T cells. *Immunol Rev* **229**, 114-125 (2009).

674

675 12. He, X. & Xu, C. Immune checkpoint signaling and cancer immunotherapy. *Cell Res* **30**, 660-
676 669 (2020).

677

678 13. Martin-Ruiz, A. *et al.* Effects of anti-PD-1 immunotherapy on tumor regression: insights from
679 a patient-derived xenograft model. *Sci Rep* **10**, 7078 (2020).

680

681 14. Lee, J. *et al.* Outstanding clinical efficacy of PD-1/PD-L1 inhibitors for pulmonary
682 pleomorphic carcinoma. *Eur J Cancer* **132**, 150-158 (2020).

683

684 15. Nowicki, T.S., Hu-Lieskovan, S. & Ribas, A. Mechanisms of Resistance to PD-1 and PD-L1
685 Blockade. *Cancer J* **24**, 47-53 (2018).

686

687 16. Jenkins, R.W., Barbie, D.A. & Flaherty, K.T. Mechanisms of resistance to immune checkpoint
688 inhibitors. *Br J Cancer* **118**, 9-16 (2018).

689

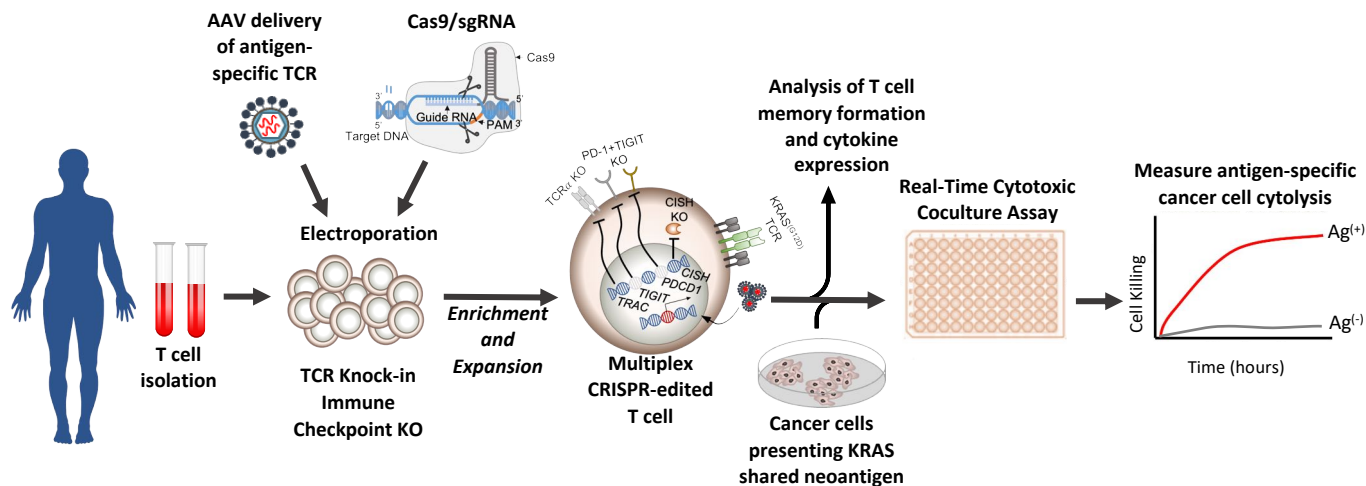
- 690 17. Sun, C., Mezzadra, R. & Schumacher, T.N. Regulation and Function of the PD-L1 Checkpoint.
691 *Immunity* **48**, 434-452 (2018).
692
- 693 18. Pawelczyk, K. *et al.* Role of PD-L1 Expression in Non-Small Cell Lung Cancer and Their
694 Prognostic Significance according to Clinicopathological Factors and Diagnostic Markers. *Int J*
695 *Mol Sci* **20** (2019).
696
- 697 19. Davis, A.A. & Patel, V.G. The role of PD-L1 expression as a predictive biomarker: an analysis
698 of all US Food and Drug Administration (FDA) approvals of immune checkpoint inhibitors. *J*
699 *Immunother Cancer* **7**, 278 (2019).
700
- 701 20. Douglas C. Palmer, *et al.* Internal checkpoint regulates T cell neoantigen reactivity and
702 susceptibility to PD-1 blockade. *bioRxiv In press* (2020).
703
- 704 21. Yoshimura, A. CIS: the late-blooming eldest son. *Nat Immunol* **14**, 692-694 (2013).
705
- 706 22. Palmer, D.C. *et al.* Cish actively silences TCR signaling in CD8+ T cells to maintain tumor
707 tolerance. *The Journal of experimental medicine* **212**, 2095-2113 (2015).
708
- 709 23. Guittard, G. *et al.* The Cish SH2 domain is essential for PLC-gamma1 regulation in TCR
710 stimulated CD8(+) T cells. *Sci Rep* **8**, 5336 (2018).
711
- 712 24. Delconte, R.B. *et al.* CIS is a potent checkpoint in NK cell-mediated tumor immunity. *Nat*
713 *Immunol* **17**, 816-824 (2016).
714
- 715 25. Zhu, H. *et al.* Metabolic Reprograming via Deletion of CISH in Human iPSC-Derived NK Cells
716 Promotes In Vivo Persistence and Enhances Anti-tumor Activity. *Cell Stem Cell* **27**, 224-237
717 e226 (2020).
718
- 719 26. Miah, M.A. *et al.* CISH is induced during DC development and regulates DC-mediated CTL
720 activation. *Eur J Immunol* **42**, 58-68 (2012).
721
- 722 27. ClinicalTrials.gov [Internet]. Bethesda (MD): National Library of Medicine
723 (US). 2000 Feb 29 - . Identifier NCT04426669, A Study of Metastatic Gastrointestinal Cancers
724 Treated With Tumor Infiltrating Lymphocytes in Which the Gene Encoding the Intracellular
725 Immune Checkpoint CISH Is Inhibited Using CRISPR Genetic Engineering; 2020 June 11.
726 Available from:
727 <https://clinicaltrials.gov/ct2/show/NCT04426669>.
728
- 729 28. Tran, E. *et al.* Immunogenicity of somatic mutations in human gastrointestinal cancers.
730 *Science* **350**, 1387-1390 (2015).
731
- 732 29. Ikebuchi, R. *et al.* Influence of PD-L1 cross-linking on cell death in PD-L1-expressing cell lines
733 and bovine lymphocytes. *Immunology* **142**, 551-561 (2014).
734
- 735 30. Chen, S. *et al.* Mechanisms regulating PD-L1 expression on tumor and immune cells. *J*
736 *Immunother Cancer* **7**, 305 (2019).
737
- 738 31. Zhao, Z. *et al.* CRISPR knock out of programmed cell death protein 1 enhances anti-tumor
739 activity of cytotoxic T lymphocytes. *Oncotarget* **9**, 5208-5215 (2018).
740

- 741 32. Lanzel, E.A. *et al.* Predicting PD-L1 expression on human cancer cells using next-generation
742 sequencing information in computational simulation models. *Cancer Immunol Immunother*
743 **65**, 1511-1522 (2016).
744
- 745 33. Boegel, S., Lower, M., Bukur, T., Sahin, U. & Castle, J.C. A catalog of HLA type, HLA
746 expression, and neo-epitope candidates in human cancer cell lines. *Oncoimmunology* **3**,
747 e954893 (2014).
748
- 749 34. Bairoch, A. The Cellosaurus, a Cell-Line Knowledge Resource. *J Biomol Tech* **29**, 25-38 (2018).
750
- 751 35. Nakayama, N. *et al.* KRAS or BRAF mutation status is a useful predictor of sensitivity to MEK
752 inhibition in ovarian cancer. *Br J Cancer* **99**, 2020-2028 (2008).
753
- 754 36. Tate, J.G. *et al.* COSMIC: the Catalogue Of Somatic Mutations In Cancer. *Nucleic Acids Res* **47**,
755 D941-D947 (2019).
756
- 757 37. Latchman, Y. *et al.* PD-L2 is a second ligand for PD-1 and inhibits T cell activation. *Nat*
758 *Immunol* **2**, 261-268 (2001).
759
- 760 38. Zhang, Q. *et al.* Blockade of the checkpoint receptor TIGIT prevents NK cell exhaustion and
761 elicits potent anti-tumor immunity. *Nat Immunol* **19**, 723-732 (2018).
762
- 763 39. Johnston, R.J. *et al.* The immunoreceptor TIGIT regulates antitumor and antiviral CD8(+) T
764 cell effector function. *Cancer Cell* **26**, 923-937 (2014).
765
- 766 40. Spranger, S. *et al.* Density of immunogenic antigens does not explain the presence or
767 absence of the T-cell-inflamed tumor microenvironment in melanoma. *Proceedings of the*
768 *National Academy of Sciences of the United States of America* **113**, E7759-E7768 (2016).
769
- 770 41. Creelan, B.C. *et al.* Tumor-infiltrating lymphocyte treatment for anti-PD-1-resistant
771 metastatic lung cancer: a phase 1 trial. *Nat Med* **27**, 1410-1418 (2021).
772
- 773 42. Xia, A., Zhang, Y., Xu, J., Yin, T. & Lu, X.J. T Cell Dysfunction in Cancer Immunity and
774 Immunotherapy. *Front Immunol* **10**, 1719 (2019).
775
- 776 43. Zhao, Y., Shao, Q. & Peng, G. Exhaustion and senescence: two crucial dysfunctional states of
777 T cells in the tumor microenvironment. *Cell Mol Immunol* **17**, 27-35 (2020).
778
- 779 44. Anderson, K.G., Stromnes, I.M. & Greenberg, P.D. Obstacles Posed by the Tumor
780 Microenvironment to T cell Activity: A Case for Synergistic Therapies. *Cancer Cell* **31**, 311-
781 325 (2017).
782
- 783 45. Egen, J.G., Ouyang, W. & Wu, L.C. Human Anti-tumor Immunity: Insights from
784 Immunotherapy Clinical Trials. *Immunity* **52**, 36-54 (2020).
785
- 786 46. Reck, M. *et al.* Pembrolizumab versus Chemotherapy for PD-L1-Positive Non-Small-Cell Lung
787 Cancer. *N Engl J Med* **375**, 1823-1833 (2016).
788
- 789 47. Chauvin, J.M. & Zarour, H.M. TIGIT in cancer immunotherapy. *J Immunother Cancer* **8** (2020).
790

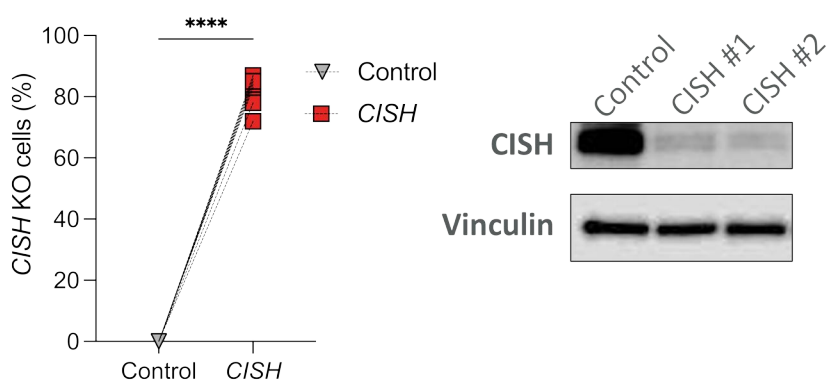
- 791 48. Solomon, B.L. & Garrido-Laguna, I. TIGIT: a novel immunotherapy target moving from bench
792 to bedside. *Cancer Immunol Immunother* **67**, 1659-1667 (2018).
793
- 794 49. Casado, J.G. *et al.* Expression of adhesion molecules and ligands for activating and
795 costimulatory receptors involved in cell-mediated cytotoxicity in a large panel of human
796 melanoma cell lines. *Cancer Immunol Immunother* **58**, 1517-1526 (2009).
797
- 798 50. Levin, S.D. *et al.* Vstm3 is a member of the CD28 family and an important modulator of T-cell
799 function. *Eur J Immunol* **41**, 902-915 (2011).
800
- 801 51. Stanietsky, N. *et al.* The interaction of TIGIT with PVR and PVRL2 inhibits human NK cell
802 cytotoxicity. *Proc Natl Acad Sci U S A* **106**, 17858-17863 (2009).
803
- 804 52. Yu, X. *et al.* The surface protein TIGIT suppresses T cell activation by promoting the
805 generation of mature immunoregulatory dendritic cells. *Nat Immunol* **10**, 48-57 (2009).
806
807

Figure 1: Multiplex CRISPR/rAAV editing of CISH and KRAS(G12D) TCR integration in primary human T cells.

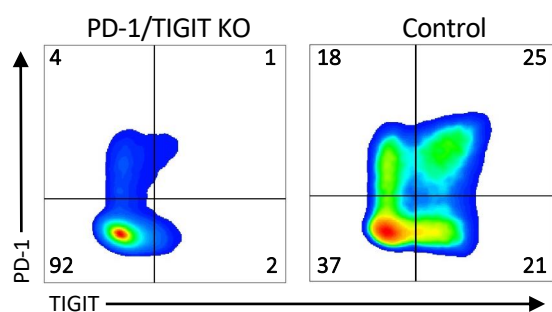
a



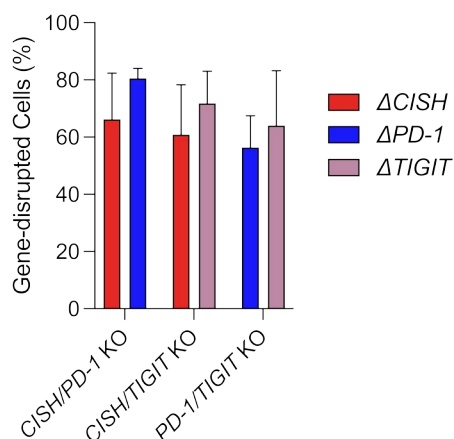
b



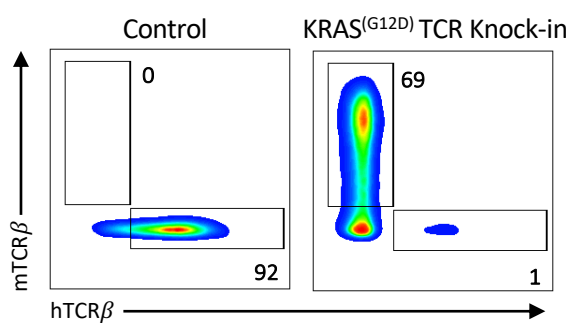
c



d



e



f

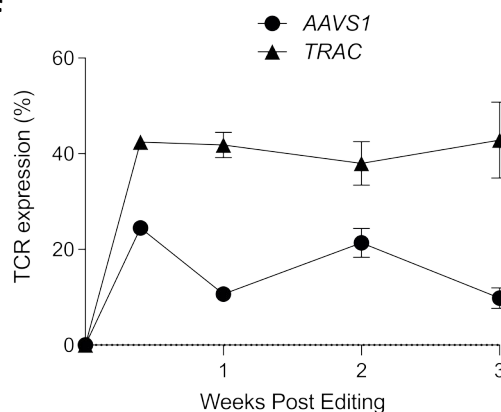


Figure 2: Inactivation of CISH in human T cells enhances T cell effector function upon TCR signaling.

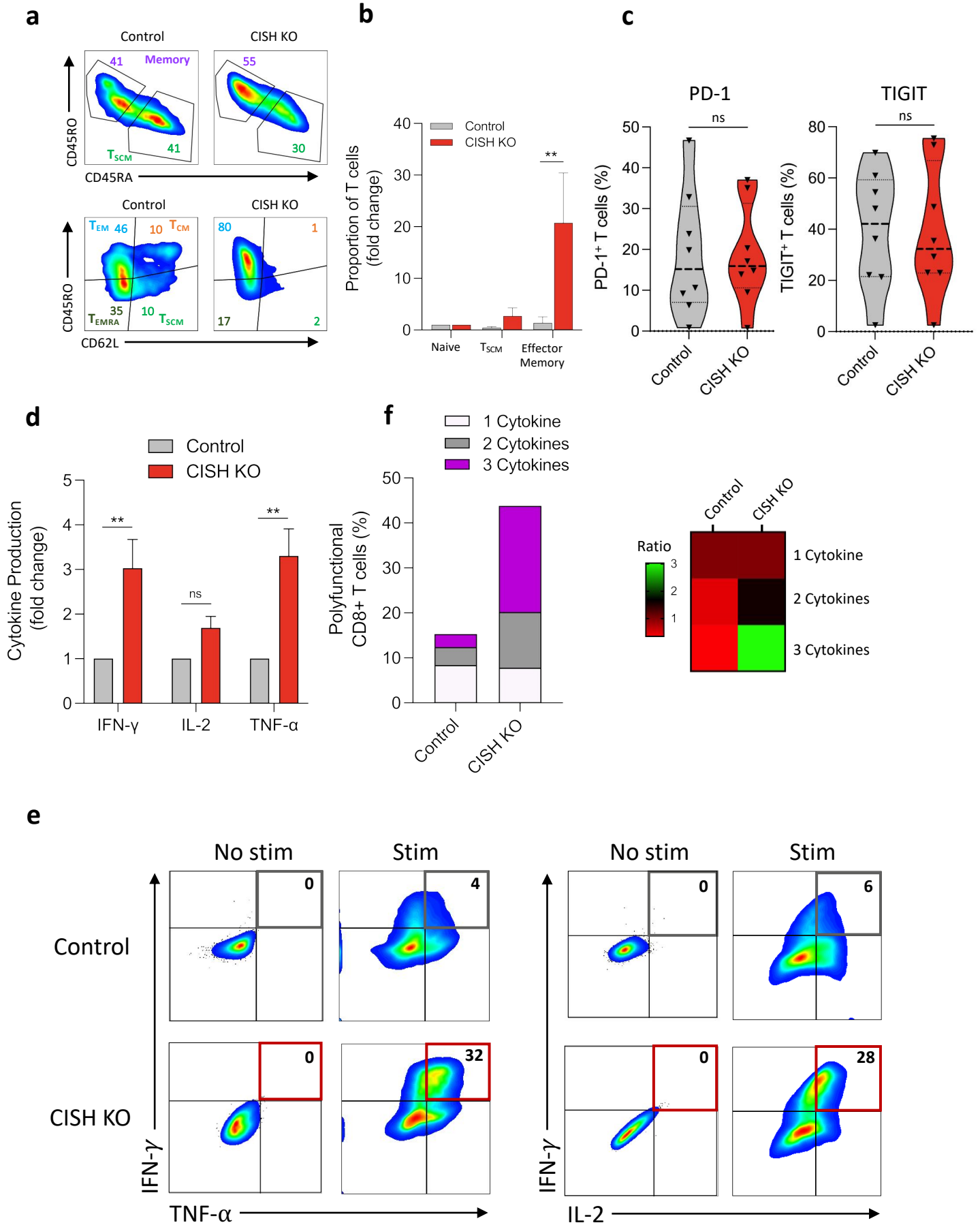


Figure 3: PD-1 or TIGIT disruption does not enhance T cell effector functions upon TCR signaling.

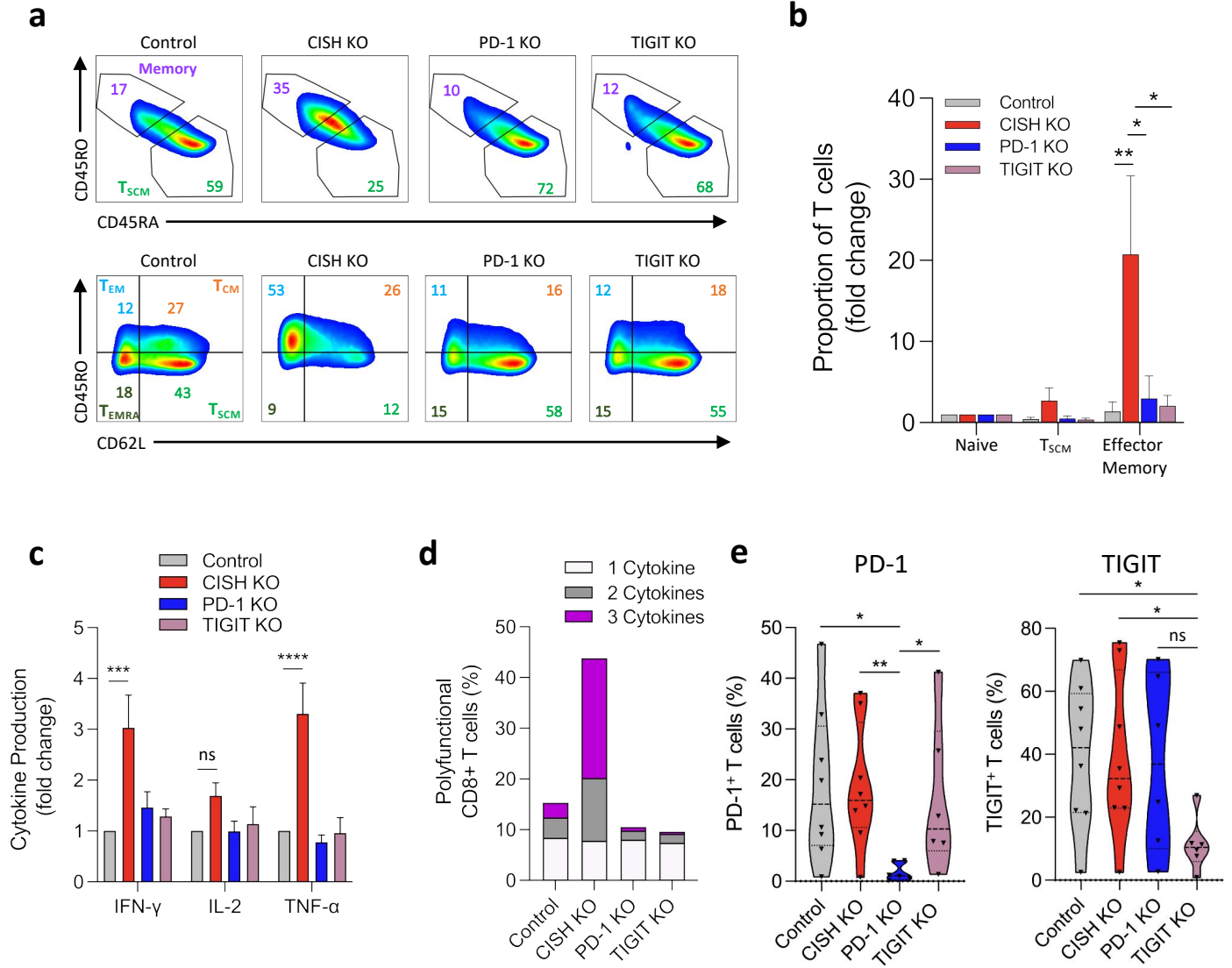


Figure 4: The increased antigen-specific cancer cell killing by CISH disrupted T cells is elevated above that seen by PD-1 deficient T cells.

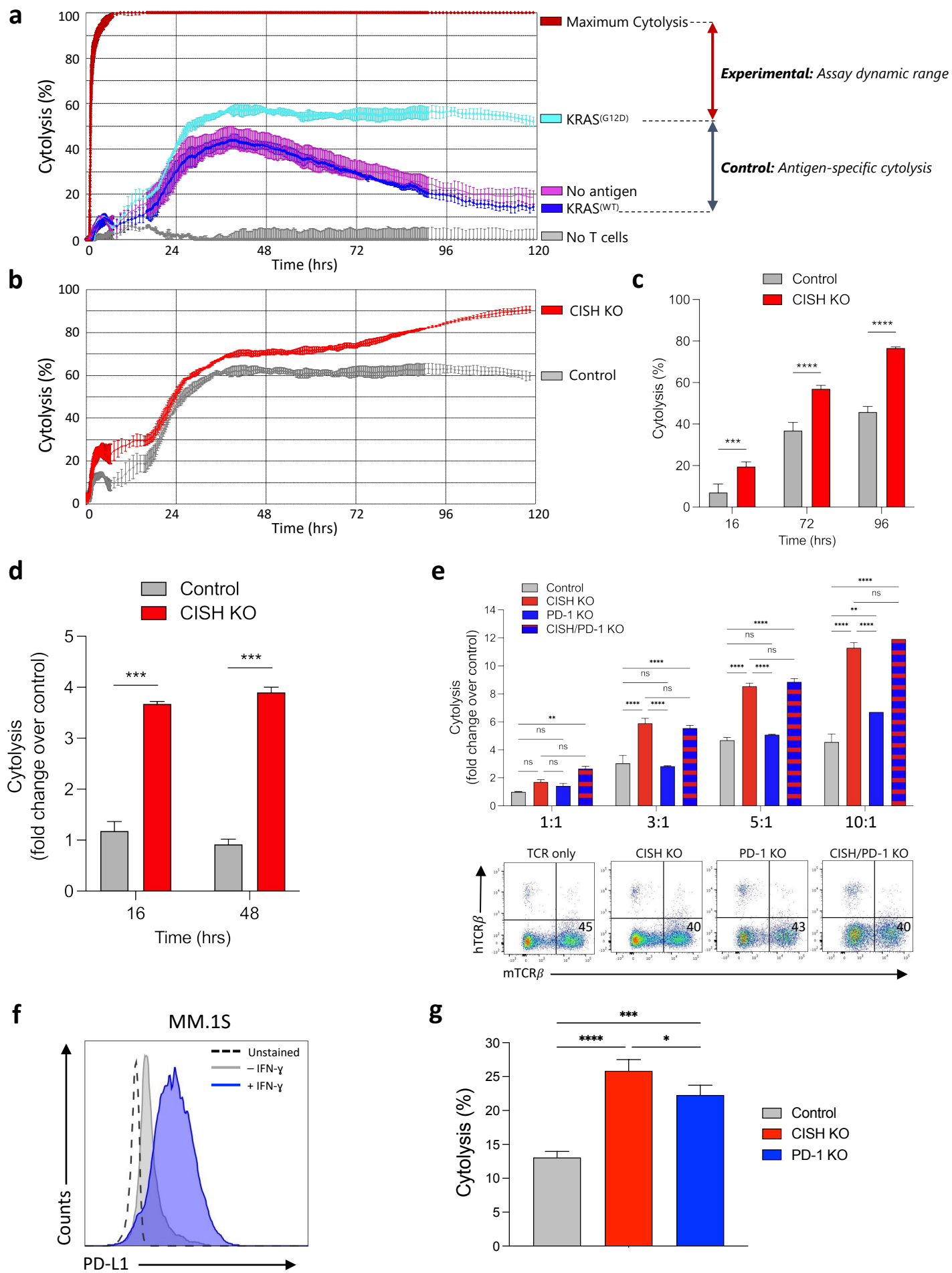


Figure 5: Enhanced antigen-specific cytolysis of PD-1 and TIGIT-deficient T cells is dependent on PD-L1 expression on the cancer cells, whereas elevated cytolysis by CISH inactivation is ligand-independent.

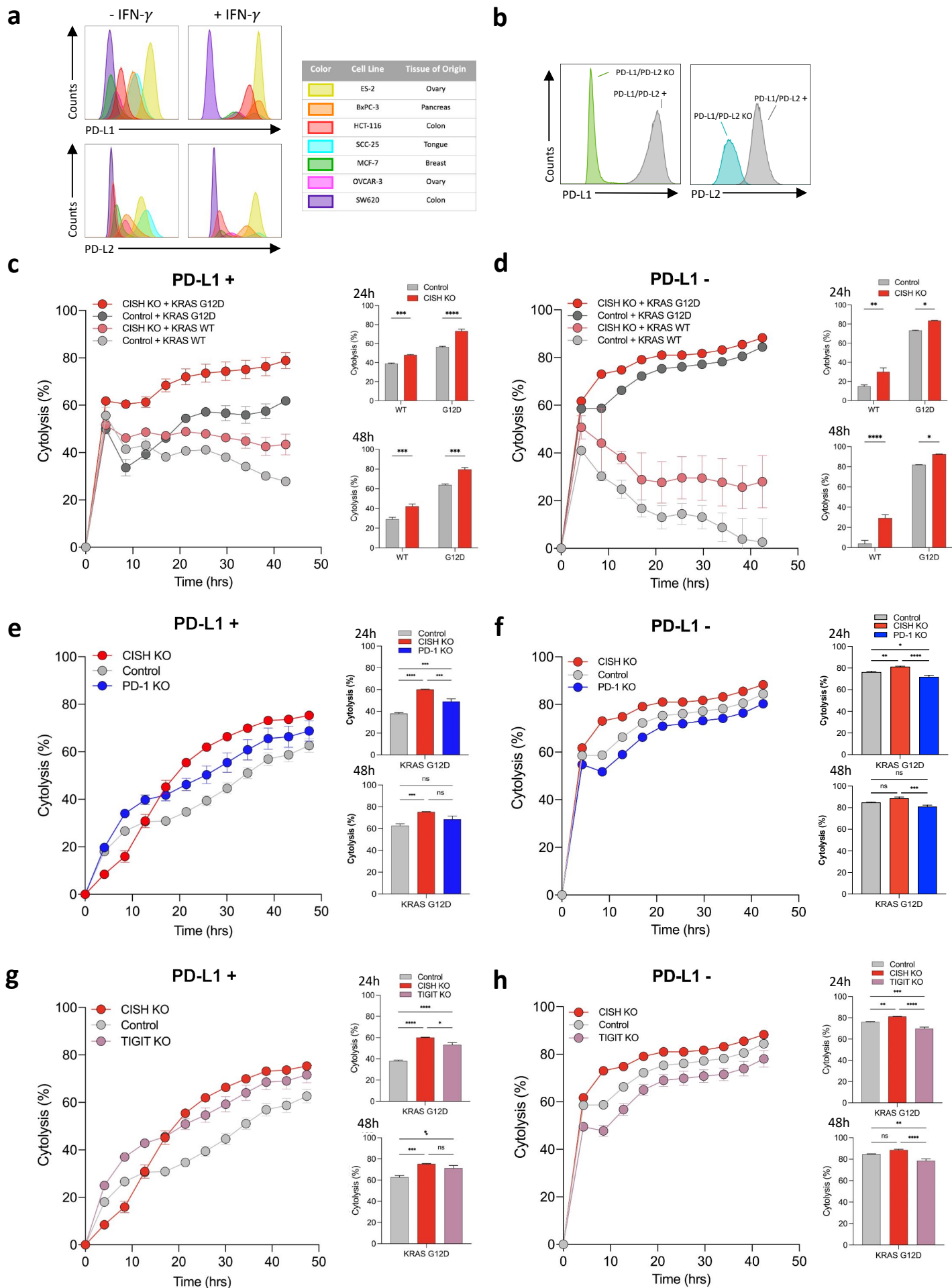


Figure 6: Inactivation of CISH and PD-1/TIGIT synergize to maximize the increase in antigen-specific cancer cell cytotoxicity.

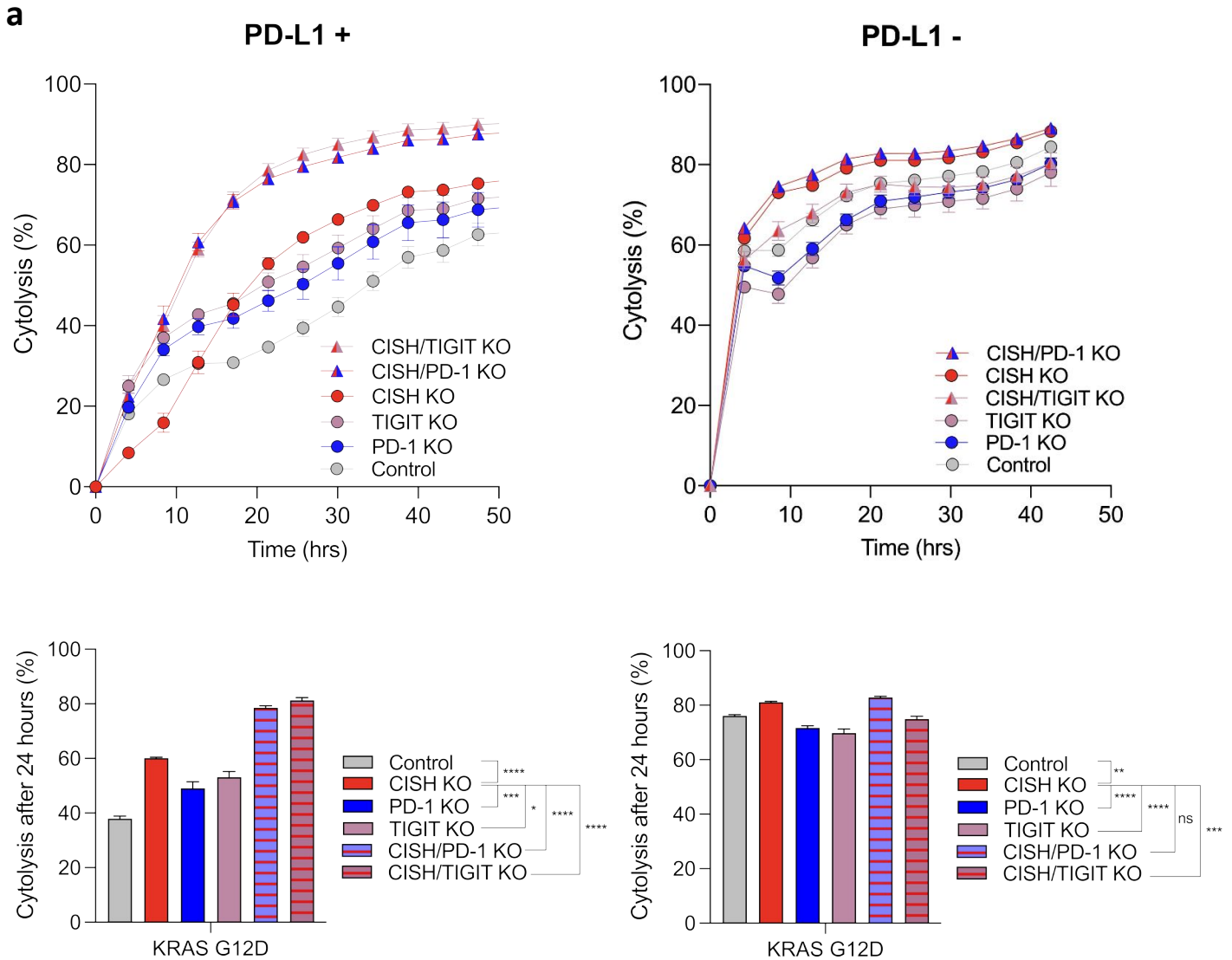


Table 1: The attributes of intra-cellular CISH inhibition in human T cells in comparison to cell surface immune checkpoints PD-1 and TIGIT.

	PD-1	TIGIT	CISH
Ligand Dependency	Ligand Dependent (PD-L1 / PD-L2)	Ligand Dependent (CD155, CD112, CD113)	Ligand Independent
Clinical Efficacy	Durable Antitumor Responses; Percentage of Responders Low ORR = 26% (Keytruda) / ORR = 40% (Opdivo)	Modest Evidence of Efficacy in Combination with Anti-PD-1	To Be Determined Currently being assessed in a clinical trial for solid tumor†
Druggability	Cell Surface - Readily Druggable With mAb	Cell Surface - Readily Druggable With mAb	Intracellular - Challenging to Drug Addressed via genetically engineered CISH KO T Cell Therapy

† <https://clinicaltrials.gov/ct2/show/NCT04426669>